EAI Endorsed Transactions
on Ai and Robotics
Research Article EAI.EU

Prediction of short circuit current of wind turbines based on artificial neural network model

Ali AbdulKarim AbdulRahim[1], Ebrahim Aghajari[2,*]

[1]Department of Electrical Engineering, Ahvaz Branch, Islamic Azad University, Ahvaz, Iran
[2]Department of Electrical Engineering, Ahvaz Branch, Islamic Azad University, Ahvaz, Iran

Abstract

The growth of renewable energy on a global scale is making significant strides in power plants. This is due to the increasing concern about climate change, the rising demand for electricity, and the necessity to reduce reliance on fossil fuels. Ensuring the successful integration of new energy resources into the existing network is just as crucial as it requires the system to be reliable and adaptable. For instance, wind energy, which is one of the renewable sources, has an intermittent nature that necessitates the ability to synchronize its actions to achieve the desired system performance. The objective of this study is to utilize a new neural network system to calculate the short circuit current of power plants. Specifically, the focus is on identifying and categorizing the short circuit faults that occur between the stator coils of the squirrel cage induction generator used in wind power generation. To achieve this, a system was developed to simulate turbine data. Subsequently, four feature extraction techniques and machine learning algorithms were employed to enable early detection of short circuit faults. The numerical results obtained from the simulation demonstrated the high efficiency and accuracy of the proposed model. This research is based on a valid approach for early detection of short circuit in the stator winding in induction generators used in wind turbines. Using a wind turbine test location, we introduced different types of short circuit in the generator. We proposed to use four feature extraction technical along with three categories.

Keywords: Power Plant, Short Circuit Current, Neural Network.

Received on 20 03 2024, accepted on 20 06 2024, published on 17 07 2024

doi: 10.4108/airo.5955

1. Introduction

Advances in technology for the optimal extraction of energy from renewable sources, along with cost reductions and government policies with financial incentives that support the growth of renewable energy, have led to a significant integration of renewable energy sources. For example, a new energy agreement was reached in Denmark in March 2012 which includes initiatives to bring Denmark closer to the goal of 100% renewable energy in the energy and transport sectors by 2050. Ontario's Green Energy and Green Economy Act of 2009 created a feed-in program that provides payment for renewable energy production above the market price. As the installed capacity of wind generation continues to grow, it is necessary for facility engineers to be aware of the behavioural characteristics of wind farms and the effects they have on the power grid, and this growth presents unique challenges for the proper integration of wind energy into the power grid [1].

A unique aspect of wind generation that separates it from conventional generation is its short circuit behaviour. Wind turbines typically use an induction generator that is either directly connected to the grid or decoupled from the grid via power electronics. These topologies have different short-circuit characteristics compared to concurrently connected machines. Appropriate short-circuit studies are necessary to determine that the maximum short-circuit contribution of a given machine is within the range of the

*Corresponding author. Email: eaghajari88@iau.ac.ir

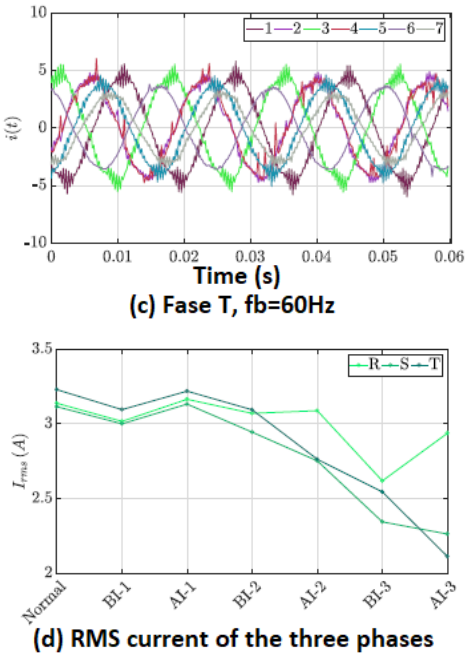

Figure 5. Comparison of the electric current of three lines, with performance close to the nominal current, in different failure conditions. Caption (1) generator in normal state, (2) failure AI-1, (3) BI-1, (4) AI-2, (5) BI-2, (6) AI-3, (7) BI-3

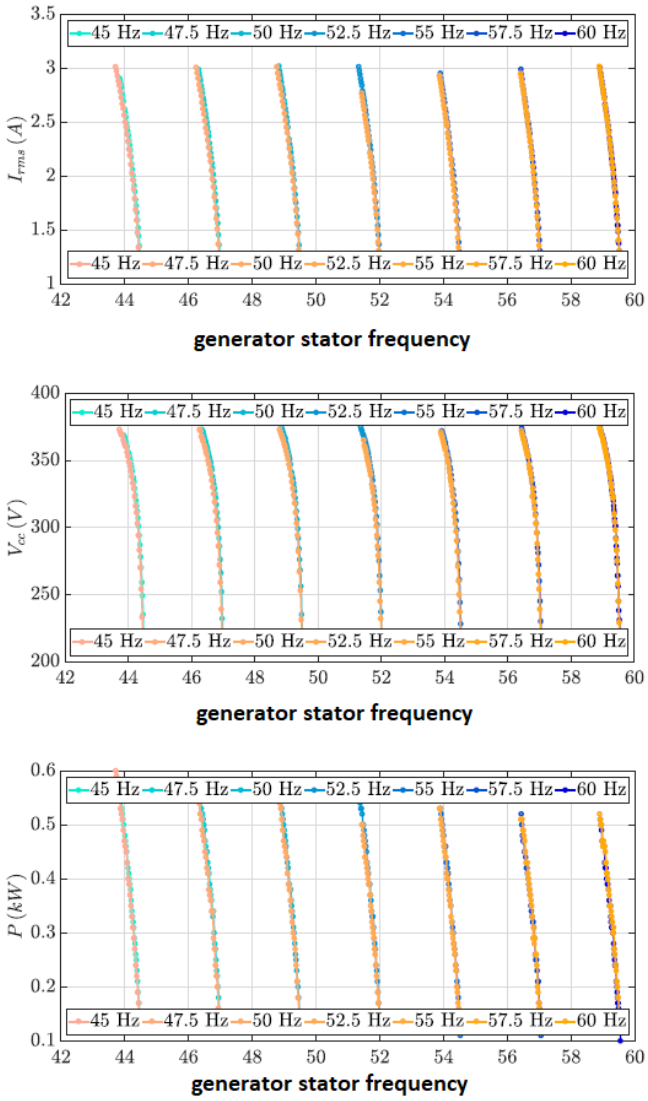

Figure 6. Corrected SCIG curves under normal conditions, in blue, and error1 CC AI-, in yellow. In 4-16A the behaviour of electric current, in 4-16B the voltage in DC Bus and in 4-16C the three-phase power is produced

Evidence of a short circuit during critical failure is noticeable in the generator curves presented in Figure 7. Bus DC voltage curves and powers are far from nominal values compared to normal conditions. However, in the event of an initial breakdown (i.e. AI-1), there is almost no difference in voltage and power, as shown in Figure 7. The power and voltage information in the DC Bus indicates the occurrence of problems in the generator, so using this information in relation to other techniques can help in identifying the failures of the induction generator.

The short circuit simulation is entered in the branch between the R and S phases and although the T phase is not short-circuited on the branch, it is believed that the appearance of a fault is perceived in all three generator currents. Feature extraction was done in phase A. Database formation is explained in the next section.

3.1. Results of applications of extractor versus classifier

Table 5 shows the general results after 50 exercises of all the extractor-classifier combinations, in the training and testing bases. Using Fourier as the feature extractor, MLP

achieved an average success rate among all classes of 84.48% and 76.53% in the training and test bases, respectively. As expected, it was better than linear classifications. Adding new features to the database provided improvements in all extractor-classifier combinations, however, it did not make the problem linearly separable, which justified the results of the OLS and Simple Perceptron classifiers reaching results below the MLP and Gaussian classifier. The sensitivity shows that MLP is better than other methods for identifying the normal operating conditions of the generator.

The feature also shows that MLP is better than other classifiers in predicting faulty conditions. Goertzel's algorithm, despite implementing Fourier transform, provided results below classical Fourier transform for MLP classifier. This is especially seen in the test base, where the difference between the results in the training and test bases is greater than that of the Fourier extractor. Obviously, with this extractor, the simple perceptron and OLS classifiers obtained much worse results than the Fourier extractor, indicating that the use of this extractor worsens the separability of the database.

Also, in Table 5, the combination of HOS-MLP ranks second in overall accuracy. There is a highlight for combining this extractor with a Gaussian classifier. This occurs because both the HOS extractor and the Gaussian classifier base their theories on Gaussian processes. The results of this extractor in linear classifiers were better than Goertzel's extractor, which indicates better resolution. SCM extractor was not effective for induction generator failure classification. Through these analyses, it was found that Fourier extractor is more effective for detecting short circuit in induction generator.

Table 5. The overall results of the extractor-classifier for the following criteria:

Accuracy (Acc), sensitivity (Sen), specificity (ESP), F score (Fsc) in training and test databases

classifier	Acc %	Sen %	ESP %	Fsc %
Training				
Fourier				
MLP	84.48 ±2.65	84.48 ±2.65	97.01 ±0.59	84.48 ±2.65
quadratic Gaussian	77.30 ±0.63	77.47 ±1.13	95.33 ±0.16	77.39 ±0.81
simple perceptron	66.56 ±1.17	67.19 ±1.71	92.43 ±0.43	67.13 ±1.37
OLS	64.91 ±0.88	65.10 ±1.03	91.73 ±0.29	65.00 ±0.87
Goertzel				
MLP	81.42 ±1.46	81.42 ±1.46	96.33 ±0.34	81.42 ±1.46
quadratic Gaussian	75.40 ±0.58	73.59 ±1.56	91.26 ±0.98	75.54 ±0.87
simple perceptron	32.80 ±2.53	33.01 ±2.71	74.66 ±2.40	33.04 ±2.73
OLS	42.48 ±0.99	42.86 ±1.19	81.64 ±0.60	42.72 ±1.03
HOS				
MLP	83.31 ±1.69	85.31 ±3.57	98.82 ±0.74	93.31 ±2.03
quadratic Gaussian	78.96 ±0.64	78.96 ±0.64	95.75 ±0.16	78.96 ±0.64
simple perceptron	49.73 ±2.61	49.75 ±2.59	85.69 ±1.54	49.91 ±2.80
OLS	59.31 ±1.26	59.67 ±1.72	89.80 ±0.51	59.58 ±1.40
SCM				
MLP	40.93 ±5.58	40.93 ±7.97	80.61 ±3.56	40.93 ±4.75
quadratic Gaussian	54.97 ±1.00	55.03 ±1.05	88.00 ±0.41	55.03 ±1.00
simple perceptron	30.75 ±1.72	31.03 ±1.71	73.21 ±1.71	31.18 ±1.64
OLS	43.62 ±0.97	43.93 ±1.36	82.34 ±0.54	43.83 ±1.08
Test				
Fourier				
MLP	76.53 ±3.45	76.98 ±3.59	95.13 ±0.87	76.79 ±3.40
quadratic Gaussian	72.32 ±2.29	72.61 ±2.42	94.09 ±0.68	72.65 ±2.36
simple perceptron	66.56 ±1.17	67.19 ±1.71	92.43 ±0.43	67.13 ±1.37
OLS	64.91 ±0.88	65.10 ±1.03	91.73 ±0.29	65.00 ±0.87
Goertzel				
MLP	65.59 ±3.16	65.59 ±3.16	92.16 ±0.94	65.92 ±2.99
quadratic Gaussian	71.30 ±0.78	70.32 ±1.21	88.57 ±0.78	71.53 ±0.54
simple perceptron	32.80 ±2.53	33.01 ±2.71	74.66 ±2.40	33.04 ±2.73
OLS	42.48 ±0.99	42.86 ±1.19	81.64 ±0.60	42.72 ±1.03
HOS				
MLP	73.54 ±1.42	73.54 ±2.31	86.82 ±0.34	73.54 ±1.57
quadratic Gaussian	76.72 ±2.13	76.94 ±2.25	95.25 ±0.59	76.97 ±2.10
simple perceptron	49.73 ±2.61	49.75 ±2.59	85.69 ±1.54	49.91 ±2.80
OLS	59.31 ±1.26	59.67 ±1.72	89.80 ±0.51	59.58 ±1.40
SCM				
MLP	57.15 ±1.52	57.24 ±1.52	88.88 ±0.62	57.20 ±1.51
quadratic Gaussian	51.49 ±2.37	52.25 ±2.87	86.73 ±1.09	52.21 ±2.42
simple perceptron	30.75 ±1.72	31.03 ±1.71	73.21 ±1.71	31.18 ±1.64
OLS	43.62 ±0.97	43.93 ±1.36	82.34 ±0.54	43.83 ±1.08

Table 6. The amount of hit according to the class of all classifiers using the Fourier extractor

Class	Training			
	MLP	quadratic Gaussian	simple perceptron	OLS
Normal	99.98± 0.11	99.14±0.33	100.00±0.00	99.81 ±0.34
AI-1	73.51± 12.26	62.94±3.27	54.05±5.85	58.51 ±4.10
AI-2	66.00± 8.74	54.11±3.28	24.68±13.85	27.86 ±5.60
AI-3	94.05± 3.82	86.71±1.31	61.57±11.78	89.68 ±1.76
BI-1	58.94± 12.36	39.49±5.91	9.51±9.82	26.30 ±0.68
BI-2	98.89± 1.12	92.10±1.21	33.29±17.12	54.08 ±3.61
BI-3	100.00 ±0.00	100.0±0.00	77.06±18.53	98.13 ±0.57
Class	**Test**			
	MLP	**quadratic Gaussian**	**simple perceptron**	**OLS**
Normal	99.25± 1.18	98.76±1.61	99.98±0.12	99.70 ±0.46
AI-1	52.16± 14.23	53.80±7.01	53.32±7.67	55.53 ±5.09
AI-2	49.96± 11.07	47.78±8.02	22.00±13.46	26.15 ±6.92
AI-3	85.58± 6.92	82.70±6.80	61.30±13.17	89.16 ±3.70
BI-1	36.94± 14.46	25.03±9.91	7.88±9.18	23.73 ±4.18
BI-2	92.44± 4.09	89.10±4.46	32.93±18.76	52.71 ±4.38
BI-3	98.81± 1.99	100.00±0.0 0	78.31±18.07	97.69 ±2.35

Table 6 shows the rate of hit based on the class of the proposed classifiers. It can be seen that in all the classifiers, the Normal class was obtained more than 98%. Class BI-3 was classified by MLP with 100% and 99.81% accuracy in training and test bases. And this was expected because this is the most critical database failure condition. Linear classifiers achieved lower success rates than MLP for other classes.

4. Conclusions

The current work deals with the prediction of wind turbine short circuit condition on the basis of neural network techniques. In fact, in all solved cases, normal conditions were classified with an accuracy above 99%, and by grouping all errors together, 100% was obtained in a dual classification. Rejection thresholds are implemented to reduce false positive and negative rates despite none of the samples being rejected. By analysing the outputs of dual neural networks, it is possible to detect when the dc bus is far from its nominal value (311 V), normal samples are usually misclassified as faulty, but the reliability of the classifier by band rejection due to classification the false positive error is maintained to avoid it. The analysis performed on the four feature extractors showed that in all the classifiers, the results of using Fourier to combine the databases are more effective, therefore, this information is relevant to perform short circuit detection in SCIG. The method used in this work proved to be efficient and can be replicated in systems already installed in wind farms as well as in a newer wind turbine. Since the frequency converters feed the new generators, this solution can also be embedded in it, creating an integrated product that is responsible for feeding, controlling and monitoring. This will certainly increase the reliability and availability of the wind farm.

References

[1] J. Shair, X. Xie, W. Liu, X. Li, and H. Li, “Modeling and stability analysis methods for investigating subsynchronous control interaction in large-scale wind power systems,” in Renew Sustain Energy Rev. vol. 135 pp. 110420, 2021.

[2] G. Rudy, and K.H. Khwee, “A new T-circuit model of wind turbine generator for power system steady state studies,” Bulletin of Electrical Engineering and Informatics. vol. 10, no.2, pp. 550-558, 2021.

[3] G.T. Enes, S. Emiroglu, and M.A. Yalcin, “Optimal DG allocation and sizing in distribution systems with Thevenin based impedance stability index,” International Journal of Electrical Power & Energy Systems, vol. 144, pp. 108555, 2023.

[4] D. Oliveira, R. Alves, and M.H. Bollen, “Susceptibility of large wind power plants to voltage disturbances-Recommendations to stakeholders,” Journal of Modern Power Systems and Clean Energy. vol. 10, no. 2. pp. 416-429, 2021.

[5] L. Trevor, “Wind energy engineering: A handbook for onshore and offshore wind turbines,” Elsevier, 2023.

[6] J.B. Francisco, “Short-circuit current contribution of doubly-fed wind turbines according to IEC and IEEE standards,” IEEE Transactions on Power Delivery. vol. 36, no. 5, pp. 2904-2912, 2020.

[7] R.M. Furlaneto, I. Kocar, A. Grilo-Pavani, U. Karaagac, A. Haddadi, and E. Farantatos, “Short circuit network equivalents of systems with inverter-based resources reference,” Electric Power Systems Research. Elsevier, vol. 199, no. 107314, 2021.

[8] F. Jimenez-Buendıa, A. Honrubia-Escribano, A. Lorenzo-Bonache, E. Artigao, and E. Gomez-Lazaro, “Short-Circuit Current Contribution of Doubly-Fed WindTurbines according to IEC and IEEE Standards,” IEEE TRANSACTIONS ONPOWER

DELIVERY. IEEE, Minneapolis, Minnesota, USA, pp. 1-10, 2020.

[9] K. Mahesh, "Optimal multi-objective placement and sizing of distributed generation in distribution system: a comprehensive review," Energies. vol. 15, no. 21, pp. 7850, 2022.

[10] A.H. Mohammadzadeh Niaki, and A.H. Solat, "A Novel Method to Determine the Maximum Penetration Level of Distributed Generation in the Distribution Network," 2020 28th Iranian Conference on Electrical Engineering (ICEE). IEEE, 2020.

[11] S.H. Abdurrahman, Y. Sun, and Z. Wang, "Optimization techniques applied for optimal planning and integration of renewable energy sources based on distributed generation: Recent trends," Cogent Engineering. vol. 7, no. 1, pp. 1766394, 2020.

[12] D. Mohammad, Z. Montazeri, and O.P. Malik, "Optimal sizing and placement of capacitor banks and distributed generation in distribution systems using spring search algorithm," International Journal of Emerging Electric Power Systems. vol. 21, no. 1, pp. 20190217, 2020.

[13] K. Eshan, "The optimal placement and sizing of distributed generation in an active distribution network with several soft open points," Energies, vol. 14, no. 4, pp. 1084, 2021.

[14] E.M. Hemmat, "Investigation of best artificial neural network topology to model the dynamic viscosity of MWCNT-ZnO/SAE 5W30 nano-lubricant," Materials Today Communications. vol. 35, pp. 106074, 2023.

[15] E.M. Hemmat, "A well-trained artificial neural network for predicting the optimum conditions of MWCNT–ZnO (10: 90)/SAE 40 nano-lubricant at different shear rates, temperatures, and concentration of nanoparticles," Arabian Journal of Chemistry. vol. 16, no. 2, pp. 104508, 2023.

[16] G.M. Mahdi, "Considering transient short-circuit currents of wind farms in overcurrent relays coordination using binary linear programming," International Journal of Electrical Power & Energy Systems. vol. 131, pp. 107086, 2021.

[17] C. Pedro, "A comprehensive overview of power converter applied in high-power wind turbine: Key challenges and potential solutions," IEEE Transactions on Power Electronics. vol. 38, no. 5, pp. 6169-6195, 2023.

[18] E.M. Hemmat, "Designing the best ANN topology for predicting the dynamic viscosity and rheological behavior of MWCNT-CuO (30: 70)/SAE 50 nano-lubricant," Colloids and Surfaces A: Physicochemical and Engineering Aspects. vol. 651, pp. 129691, 2022.